Bioorganic & Medicinal Chemistry Letters xxx (xxxx) xxxx

Contents lists available at ScienceDirect

Bioorganic & Medicinal Chemistry Letters

journal homepage: www.elsevier.com/locate/bmcl

Efficient synthesis and cell migration inhibitory effect of substituted benzamidothiazolylpyrazole-capped AWD*I-NH_2

Mian Yang[a,1], Jun Chen[a,1], Wancai Peng[a], Qiqi Li[a], Hui Shao[a], Guanping Tang[a], Tong-Cun Zhang[b], Yoshikazhu Takada[c], Long Ye[a,*], Xing-Hua Liao[b,*]

[a] Department of Chemistry, School of Chemistry and Chemical Engineering, Wuhan University of Science and Technology, Wuhan, Hubei 430081, PR China
[b] School of Life Sciences and Health, Wuhan University of Science and Technology, Wuhan, Hubei 430081, PR China
[c] Department of Dermatology, Biochemistry and Molecular Medicine, University of California Davis, School of Medicine, Sacramento, CA, United States

ARTICLE INFO

Keywords:
Cell migration
Inhibition
Peptidomimetics
Synthesis
f-Actin

ABSTRACT

Substituted (2-benzamidothiazol-5-yl)pyrazole-capped AWD*I-NH_2 were synthesized and their antimigration activity was studied. The improved efficiency and scalability of the analog synthesis was achieved via a late-stage diversification of the benzoyl group and a convergent route in which the bisazole capping agents and off-resin peptide AWD*I-NH_2 were prepared in parallel and coupled together in solution at the last step. Bioassay results indicate that all the peptidomimetics can significantly inhibit the migration of breast cancer cells MDA-MB-231 but possess no apparent cytotoxicity. In general, the antimigration potency of the peptidomimetics is correlated to the electron-withdrawing capacity of the substituents on the terminal phenyl ring. The inhibitory effect shows dose-dependent and holds also against lung and cervical cancer cells. The level of f-actin was reduced dramatically in cells treated with the inhibitor, suggesting that the migration inhibitory effect is related to the disruption of cell locomotive protrusions.

The blockade of metastasis is crucial for the treatment of cancer. As metastasis occurs at the late stage of cancer, tumor cells migrate and invade from their primary site to patient's other healthy tissues, causing serious or even lethal detriment to the patient's multiple organs and also diminishing the opportunity for site-targeting treatments such as surgical operation and radiotherapy etc. Indeed, nearly ninety percent mortality of cancer patients is attributable to the metastatic spread of the disease rather than to the primary tumor.[1–3] Therefore an anti-metastatic treatment could be a very useful disease-controlling strategy as it could stop the spread of cancer cells, reduce tissue damage caused by the invading cells and even lock the tumor at its primary site to allow for a clean removal of the tumor.

Cell migration inhibitors ideally could materialize the antimetastatic treatment as they could suppress cell motility and even keep tumors static specifically by interfering with cellular migration machinery. The last two decades have seen many migration inhibitors, either isolated from natural sources or synthetized in laboratories. These inhibitors include natural products such as (+)-migrastatin,[4] stylissamide X,[5] (+)-fusarisetin A,[6] withaferin A,[7] prodigiosin[8] and migracins A and B,[9] and synthetic compounds like thiazole derivatives as a fascin inhibitor[10] and isoxazolines as an integrin antagonist and so forth.[11–15] (+)-Migrastatin especially attracted a wide-spread interest because further development based on its core macrocyclic structure actually led to the invention of potent antimetastatic agents that are effective in vivo.[16–18] Encouraged by the progress in the area of migration inhibitors and good biocompatibility of peptidomimetics, we did a further study on a hit compound **7a**, which is a peptidomimetic migration inhibitor and an antagonist against the protein–protein interaction between lipase $sPLA_2$-IIA and integrin αvβ3.[19] The further study indicates that **7a** and its analogs can significantly inhibit not only $sPLA_2$-IIA-induced cell migration but also intrinsic migratory capacity without effecting substantial cytotoxicity. In addition, this type of peptidomimetics can also inhibit the migration of multiple other cancer cell lines, showing a good potential as a broad-spectrum antimetastatic therapeutic agent. Herein we report the details of these exciting results.

To access **7a** and its analogs efficiently and at an increasable scale, we introduced the diverse 2-benzamido groups onto the thiazole ring at the late stage of the synthesis of the bisazole capping agent **6** and coupled the agent with peptide AWD*I in solution (Scheme 1). To achieve the late-stage diversification, the amino group of the starting material (**1**) has to be protected first and deprotected later for amidation after the pyrazole ring was constructed. Initially the protection

* Corresponding authors.
E-mail addresses: yelong@wust.edu.cn (L. Ye), xinghualiao@wust.edu.cn (X.-H. Liao).
[1] These two authors contribute equally.

https://doi.org/10.1016/j.bmcl.2019.126914
Received 1 October 2019; Received in revised form 5 December 2019; Accepted 16 December 2019

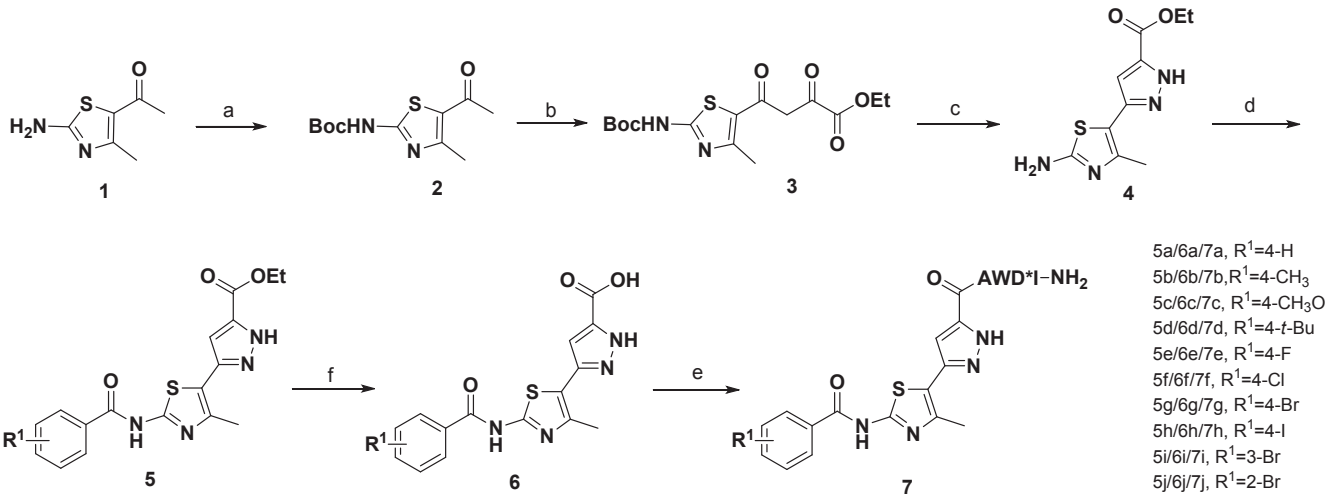

Scheme 1. Synthesis of Substituted Benzamidothiazolylpyrazole-capped AWD*I-NH_2. Reagents and conditions: (a) $(Boc)_2O$, DMAP(cat.), TEA, THF, 70 °C, 100% (b) Diethyl oxalate, LHDMS, THF, −78 °C, 84% (c) i) hydrazine hydrate, EtOH, 90 °C; ii) TFA, DCM, r.t., 73% (d) (R^1)$PhCO_2H$, CDI, DMF, 85 °C, 75–85% (f) i) NaOH (1 M, a.q.), THF, r.t.; ii) HCl (1 M, a.q.), 70–80% (g) AWD*I-NH_2, HATU, DIEPA, DMF, 0 °C-r.t. 48 h, 40–50%

reaction suffered a low yield when just Boc anhydride and a base were mixed with the amine **1** in a solvent. After several trials with reaction conditions, we found that addition of a catalytic amount of DMAP and refluxing the reaction mixture could push the protection reaction go complete, giving the *N*-Boc 2-amino thiazole derivative **2** in a quantitative yield. Then the 5-acyl group of **2** was reacted with diethyl oxalate via a Claisen condensation to form diketone **3** in a good yield. The diketone then was condensed with hydrazine hydrate to generate a pyrazole intermediate, which was subjected to solvent removal and TFA treatment to cleave the Boc group attached to the 2-amino group on the thiazole ring, resulting in **4**. The amino group of **4** was then reacted with a series of substituted benzoic acids respectively to yield substituted benzamidothiazolylpyrazoles **5**. Saponification of the ester group of **5** and subsequent acidification of the reaction mixture gave the carboxylic acids **6** in the form of off-white precipitates. Each of these acids then was reacted with the amino group of the alanine in the peptide AWD*I-NH_2 via a HATU-mediated amidation in solution phase, delivering the final products **7** in the yield of 40–50%, which is a significant increase in comparison to the very low yield of the solid-phase coupling with resin-bound AWD*I-NH_2.[19] Initially the peptide even failed to react with acids **6** under the same condition as the one for the DIC/HOBt-mediated synthesis of **7a** using the resin-bound peptide. The initial failure might be because the peptide folded with more freedom after it was cleaved off from the resin beads and its low energy conformation was able to form, resulting in a less accessible amino group of the alanine in the molecular form of the peptide versus the resin-bound peptide. After several rounds of experiments with different acyl-activating agents, it turns out that HATU could successfully mediate the formation of the peptide-bisazole conjugate (**7**). Now that the peptidomimetics do not have to be made with the resin-bound peptide as before, the production of these compounds is no longer restricted by the loading limit of the resin and it could be carried out at any desired scale. Besides the late-stage diversification of the biszaole capping agents **6** and the solution-phase reaction between the capping agent and the tetrapeptide, the above six-step synthesis of the peptidomimetics also has several other advantages over our original on-bead synthesis of the original hit (**7a**).[19] One of the advantages is the improvement of overall yield of the peptidomimetics due to the convergent synthetic route in which **6** and the peptide were prepared separately and coupled together at a final step. And the amount of acids **6** was much reduced for the final coupling reaction whereas they had to be excessive when reacting with the resin-bound peptide. Furthermore, the cryogenic Claisen condensation needs to be executed only once in the synthesis of the whole set of the analogs, whereas it would be repeated many times if various 2-benzamidothiazoles were made first and then the dry ice-chilled reaction would be run each time to form the pyrazole ring for every different analog. In all words, the synthesis of the peptidomimetics was much streamlined in comparison to the previous linear route.

To evaluate the effect of the peptidomimetics **7** on cancer cell migration, we started with a transwell assay using a highly metastatic cell line, the breast cancer cells MDA-MB-231 as a test subject in the presence of these compounds and lipase $sPLA_2$-IIA as a chemotaxi agent. Based upon the reduction of migrating cells in the presence of each of compounds **7**, we obtained the rates of inhibition on the lipase-directed cell migration by the compounds (the magenta markers in Figure 1).[20] As Figure 1 shows, the peptidomimetics **7a** through **7i** have various inhibition rates, ranging from 10% to 42%. Among the active analogs **7e** have an inhibition rate larger than the initial hit **7a**, indicating that the 4-fluorine substituent on the phenyl ring could enhance the inhibitory effect of the peptidomimetic structure. Considering the fact that a fluorine atom is much more electronegative than hydrogen but comparable in size with hydrogen, it seems that the inhibitory effect

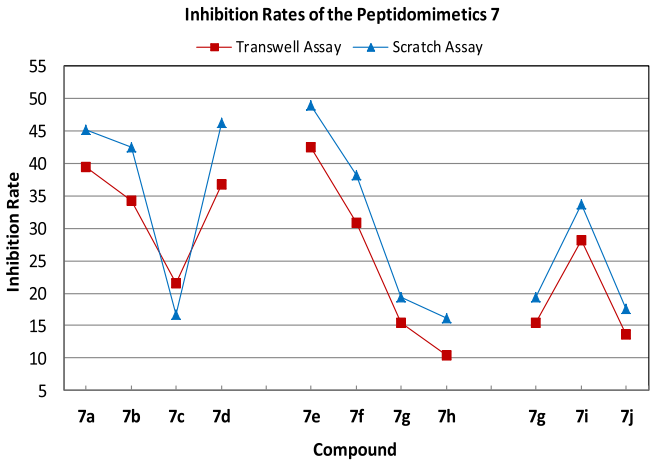

Figure 1. Inhibition rates of substituted (2-benzamidothiazol-5-yl)pyrazole-capped AWD*I(NH_2) on the motility of breast cancer cells MDA-MB-231 in both transwell and scratch assay. Cells were dosed with the DMSO solution of **7a** through **7j**, respectively. The concentrations of the compounds are 2 μM in the transwell assay and 20 μM in the scratch assay respectively.

might benefit more from the stronger electron-withdrawing ability of the fluorine substituent. On the other side, electron-donating groups such methyl, methoxy and *t*-butyl reduce the migration inhibitory potency as demonstrated by decreased inhibition rates of analog **7b** through **7d**. Especially, as methoxy is the strongest electron-donating among the three substituents, the inhibition rate of the methoxy-substituted analog (**7c**) reaches the lowest within the three analogs. Among the halogenated analogs **7e** through **7h**, the inhibition rate decreases continuously as the periodic number of the halogen substituent increases, implying that the smaller and more electron-withdrawing halogen substituent could enhance the inhibitory effect on cell migration, whereas the larger and less electron-withdrawing one would undermine the effect. Among the three brominated analogs (**7g, 7i** and **7j**), **7i** has the largest inhibition rate, meaning that the bromine substitution at the phenyl meta position is beneficial to the inhibition potency. The better activity of the *meta*-bromo substituted analog might be due to bromine's stronger electron-withdrawing force at the phenyl meta position than at para or ortho positions.[21] Considering the above structure–activity relationships, it seems that the electron-withdrawing capacity of the substituent could be the potency-increasing factor for the peptidomimetics with the same type of substituents. One of the consequences with a stronger electron-withdrawing substituent on the phenyl ring is the increased acidity of the adjacent benzamide group, making it a better hydrogen donor, which might render a stronger binding with a target protein and possibly a higher level of antimigration activity. This kind of correlation between the acidity of an amide group and the antimigration potency of the whole molecule was also observed among the isoxazoline-based cell migration inhibitors.[11] In addition, the results of the inhibition rates also indicate that there might be some other factors that could influence the potency of the migration inhibitors because the chlorinated analog **7f** is less active than the methylated one **7b** even through a chlorine atom is more electron-withdrawing than a methyl group and comparable in size with the group. One plausible reason is that a chlorine atom and a methyl group differ not only in electron-withdrawing capacity but also in some other electrosteric aspects such as static field and shape etc. More in-depth study is needed to understand the structure–activity relationship of these compounds.

To confirm the antimigration effect of the peptidomimeitcs in a different setting, we performed a scratch assay with the same line of cancer cells without using lipase $sPLA_2$-IIA to induce cell migration. Based on the reduction in the area recovered by dosed cells in comparison to the undosed ones in the absence of the chemotaxi agent, we acquired the rates of inhibition on cells' spontaneous migration by the compounds **7** (the blue markers in Figure 1).[22] As the blue markers show, all the peptidomimetic analogs have significant inhibition rates (15–49%) against cell migration even though no exogenous chemotaxi agent was added. These data suggest that the compounds could take effect on the intrinsic cellular motility as well. Also the scratch inhibition rates of **7** show the same trend as the transwell inhibition rates of these compounds. For example, the analog with the 4-methoxy substituent remains the least active among the alkyl and alkoxy substituted analogs (**7a** through **7d**). Also the fluorinated analog **7e** still has the strongest potency among all analogs. And the scratch inhibition rate also decreases from **7e** through **7h** as the periodic number of the halogen substituent increases. At last, the analog with the 3-bromo substituent also has a larger inhibition rate than the other bromo analogs in the scratch assay. However, there still are some differences between the two inhibition rates. One difference is that the scratch inhibition rates of the most analogs are larger than the transwell ones. This might be due to the higher concentration of the compounds tested in the scratch assay. The larger inhibition rates at the higher concentration of the most analogs imply that there might be a good correlation between the migration inhibition and the concentration of the peptidemimetics.

To rule out the possibility that the antimigration activity of the peptidomimetics **7** is attributable to their cytotoxicity, we performed a cell viability assay to check if there is a correlation between the two effects on cells. By comparing the amount of a metabolite generated by life dosed cells with the amount of the same metabolite by life undosed cells, we obtained the cell viability in the presence of compounds **7** (Figure 2).[23] The figure indicates that cells treated with all of the compounds at 1 μM concentration had no significant loss in viability, meaning these compounds affect little toxicity to the breast cancer cells at the concentration. The viability decreased as the concentration of the compounds was increased up to 10 μM. However, most analogs except **7j** still imposed no significant toxicity since their viability values remain around 90%. And the most potent migration inhibitors (**7e**) did not affect any viability loss at both concentrations. The other analogs such as **7a** and **7d** did not have their cell viability significantly reduced either. The most toxic analog is **7j**, which reduced cell viability by almost 30% at 10 μM, is the least potent inhibitors. Therefore, the cytotoxicity of the compounds is not correlated with their migration inhibition capacity. Therefore, the migration inhibitory effect of these compounds is least likely due to their cytotoxicity.

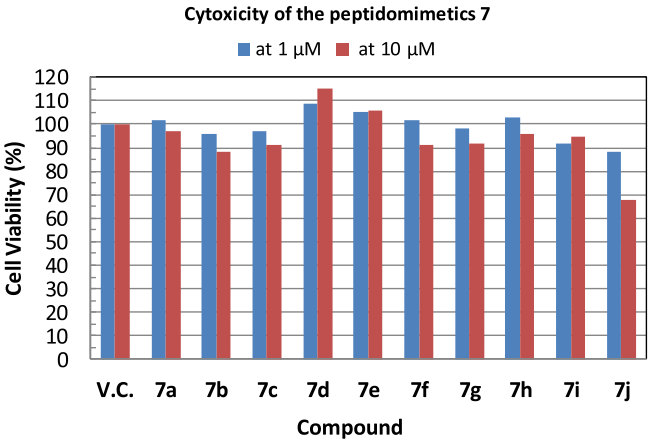

Figure 2. The cell viability of MDA-MB-231 cells in the presence of the peptidomimetics **7**. It was measured with CCK8-kit after cells were dosed with the DMSO solution of the **7a** through **7j**, respectively, or neat DMSO as a reference (V.C.) and then incubated for 48 h.

After the antimigration effect of peptidomimetics **7** were confirmed in the above assays, we then checked if the effect was specific to the breast cancer cells. Since compound **7e** has the most potency and no apparent cytotoxicity, we run a transwell migration assay with two other metastatic cells, such as lung cancer cells A549 and cervical cancer cells HELA using the same assay parameters as with the breast cancer cells. In the assay the A549 and HELA cells were dosed with the DMSO solution of the compound and cells in a control well were treated with the same volume of neat DMSO solution as of the compound solution. After all the cells were incubated as in the previous transwell assay, the cells that migrated into the lower chamber were counted. The percentage ratio of the cell counts of dosed migrating cells to that of the migrating cells in the control well were calculated and shown as relative migration rates in Figure 3. As shown in the figure, the relative migration rates of both A549 and HELA cells were reduced to about 60% of the one of the vehicle control after the cells were dosed with compound **7e**, meaning the compound can significantly inhibit the migration of both cancer cells by about 40%, which is a comparable potency as in the assay with the breast cancer cells. Also, our previous work indicates that **7a** could stop cells U937 from migrating.[19] Therefore, as this type of the compound demonstrated the inhibitory effect on migration of at least the four lines of cancer cells in total, it would serve as a valuable lead structure for the development of antimetastatic therapeutics against a broad spectrum of cancers.

As compound **7e** demonstrated the strongest inhibitory effect on cell migration in the previous assay, we chose this compound to study the

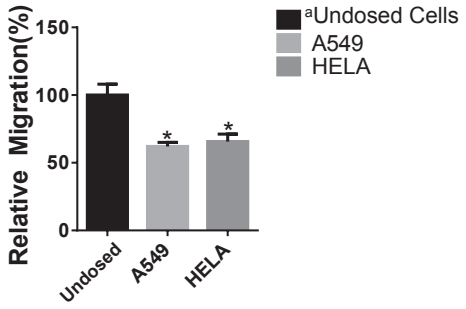

Figure 3. The relative migration of two different cancer cells, A549 and HELA in the presence of **7e**, of which concentration is 5 μM. Neat DMSO in place of the compound solution as a reference. [a]Undosed A549 or HELA cells, *: $p < 0.05$ verse control.

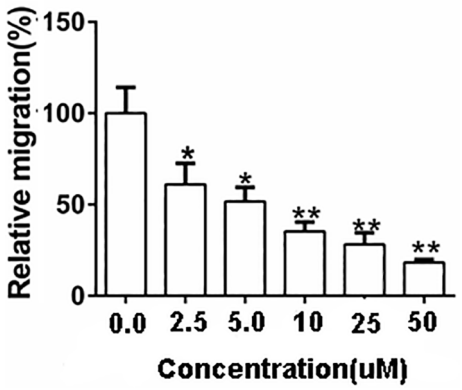

Figure 4. The result of the dose–response experiment with **7e**. The cells were dosed with the compound at different concentrations, respectively. Cellular relative migration decreases as the concentration of **7e** increases. Statistical analysis of different concentration cell migration levels. *: $p < 0.05$ verse control, **: $p < 0.01$ verse control.

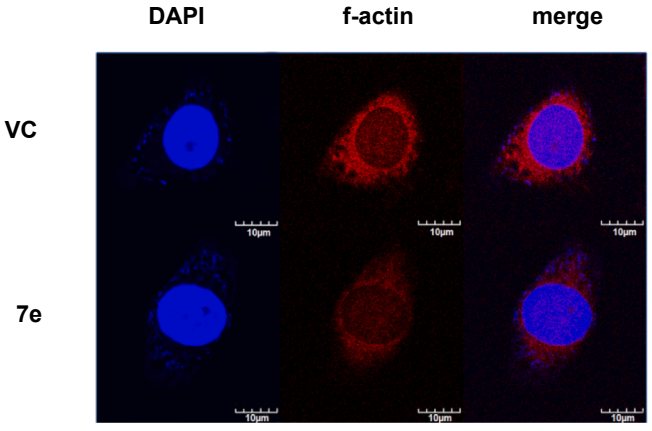

Figure 5. The microscopic images of localization of DAPI (blue) on cell nucleus and phalloidin on f-actin (red) in MDA-MB-231 cells treated with compound **7e** or DMSO vehicle control (VC). (For interpretation of the references to color in this figure legend, the reader is referred to the web version of this article.)

dose–response correlation to see how the effect varies with the concentration of the inhibitor. In this study we performed a transwell assay still with the breast cancer cells MDA-MB-231 and dosed them with a DMSO solution of the compound at a series of different concentrations. Again in a control well was just added the same volume of neat DMSO as of the compound solution. After incubation as before, only the cells that moved into the lower chamber were counted. Relative migration rates for all concentrations were obtained by calculating the percent ratio of the counts of dosed migrating cells to the count of the migrating cells in the control well (Figure 4). As shown by the figure, the relative migration rate of the cancer cells decreases continuously from about 100% to about 20% as the concentration increases from 0.0 μM to 50 μM. That is to say that the higher dose of the compound, the less cells migrated and the stronger inhibitory effect of the compound. Therefore, the migration inhibitory effect of the peptidomimetics is constantly in action as long as the dose of the compound is not zero and the inhibitory intensity is proportional to the dosage. Accurate mathematic correlation equation will be established later in a more refined experiment. Here the figure indicates that the IC_{50} of the migration inhibitor is around 5.0 μM.

To preliminarily investigate the mechanism underlying the antimigration effect of the peptidomimetics, we checked whether the level of f-actin in MDA-MB-231 cells was changed after cells were dosed with the compound **7e** as it is a key molecular assembly for cell's locomotive protrusions such as lamellipodia during cell migration.[24] In this assay f-actin in the cells that were or were not treated with compound **7e** was visualized with red Alexa548-phalloidin as shown in Fig 5.[25] The figure shows that the red color in the **7e**-dosed cells is much thinner than in the vehicle control, meaning less f-actin formed in the cells dosed by the migration inhibitor **7e**. Therefore under the influence of the peptidomimetic compound the cells could not form locomotive protrusions due to the lack of f-actin, resulting in the loss of cellular motility.

In summary, we achieved the efficient and scalable synthesis of the substituted benzamidothiazolylpyrazole-capped AWD*I-NH_2 via the late-stage diversification and solution-phase coupling between the bisazole capping agent and the peptide motif. Most of the analogs have the antimigration activity as the initial hit does but their potencies vary with the substitution on the terminal phenyl ring. In general, electron-withdrawing substituent could enhance the potency. Also, the migration-inhibiting effect of this type of compound holds against multiple cancer cell lines and most active peptidomimetics showed no apparent cytoxicity, suggesting its good potential for the development of antimetastatic therapeutics. The migration inhibitory effect is partially linked to the reduction in f-actin. More effort involving target identification is taken to investigate the detailed molecular mechanism of the antimigration effect.

Acknowledgments

Thanks are given to Overseas Scholar Starting Fund by China Education Minister (Batch 48), Natural Science Fund of Hubei Province (2015CFB490) and Open Fund of China Education Minister Key Laboratory for Medical Polymers at Wuhan University (20160101). Special thanks are given to Professor Xian-Zheng Zhang and Professor Si-Xue Cheng at Wuhan University for their generous technical suggestions and financial support. The authors also would like to thank Professor Yi Liu and Qiang-hui Zhou at Wuhan University for providing assistance in high resolution mass spectrometric analysis.

Appendix A. Supplementary data

Supplementary data to this article can be found online at https://doi.org/10.1016/j.bmcl.2019.126914.

References

1. Chambers AF, Groom AC, MacDonald IC. *Nature Rev. Cancer.* 2002;2:563.
2. Fidler IJ. *Nature Rev. Cancer.* 2003;3:453.
3. Hanahan D, Weinberg RA. *Cell.* 2011;144:646.
4. Nakae K, Yoshimoto Y, Sawa T, et al. *J. Antibiot.* 2000;53:1130.
5. Arai M, Yamano Y, Fujita M, Setiawan A, Kobayashi M. *Bioorg. Med. Chem. Lett.* 1818;2012:22.
6. Xu J, Caro-Diaz EJE, Lacoske MH. *Chem Sci.* 2012;3:3378.
7. Lee J, Hahm ER, Singh SV. *Carcinogenesis.* 1991;2010:31.
8. Zhang J, Shen Y, Liu J, Wei D. *Biochem. Pharmacol.* 2005;69:407.
9. Arai Y, Iinuma H, Ikeda Y, et al. *Antibio.* 2013;66:225.

10. (a) Zheng S, Zhong Q, Jiang Q, et al. *ACS Med. Chem. Lett.* 2013;4:191
(b) Zheng S, Zhong Q, Xi Y, et al. *J. Med. Chem.* 2014;57:6653.
11. Pitts William J, Wityak John, Smallheer Joanne M. *J. Med. Chem.* 2000;43:27.
12. Elsayed HE, Akl MR, Ebrahim HY, et al. *Chem. Biol. Drug Design.* 2015;85:231.
13. Carriero MV, Ciliberto G, Bifulco K, Pessi A. *PCT Int. Appl.* 2017;WO2017178333:A1–20171019.
14. Skruber K, Chaplin KJ, Phanstiel O. *J. Med. Chem.* 2017;60:8606.
15. Nandakumar N, Muthuraman S, Gopinath P, Nithya P, Gopas J, Kumar RS. *Euro. J. Med. Chem.* 2017;125:1076.
16. Njardarson JT, Gaul C, Shan D, Huang XY, Danishefsky SJ. Discovery of potent cell migration inhibitors through total synthesis: lessons from structure-activity studies of (+)-migrastatin. *J. Am. Chem. Soc.* 2004;126:1038.
17. Gaul C, Njardarson JT, Shan D, et al. *J. Am. Chem. Soc.* 2004;126:11326.
18. Shan D, Chen L, Njardarson JT, et al. *Proc. Natl. Acad. Sci. USA.* 2005;102:3772.
19. Ye L, Dickerson T, Kaur H, et al. *Bioorg. Med. Chem. Lett.* 2013;23:340.
20. Cells were first seeded into the upper Boyden chamber at a density of 1.0×10^5 in a media free of serum. To the lower chamber were added 10% FBS and 2.5 nM $sPLA_2$-IIA. Then the cells were dosed with the DMSO solution of compound 7 or neat DMSO as a reference in a control well. After the cells were incubated in 5% CO_2 at 37°C for 12 hours, cells which migrated into the lower chamber were counted under a microscope. The percentage ratio of the difference between the cell count of the reference and the one of the dosed cells to the cell count of the reference was calculated as the transwell inhibition rate of an individual compound (the magenta markers in Figure 1).
21. Ritche CD, Sager WF. *Prog. Phys. Org. Chem.* 1964;2:323.
22. Cells were seeded into 12-well plates and grown to about 80% confluence on the bottom of each well. Then micropipette tips were used to make a cell-free scratch on the bottom. Washed off suspended cells with PBS buffer followed by addition of a regular serum and the DMSO solution of one of the compounds **7** or neat DMSO in a control well. Then all the cells were incubated in 5% CO_2 at 37°C for 48 h. The scratch areas were covered again by migrating cells during the incubation. The percentage ratio of the difference between the area newly covered by the dosed cells and the one by the reference cells to the area newly covered by the reference cells was calculated for each compound as the scratch inhibition rate of the compound (the blue markers in Figure 1).
23. MDA-MB-231 cells were placed in a 96-well plate at the density of 1.0×10^5 and then treated with the DMSO solution of one of the compounds **7** or neat DMSO in a control. After 48 hours of incubation, cells were dosed with compound WST-8 from a CCK-8 kit and incubated for another 1 hour and then the optical density (OD) value of the cellular metabolite of WST-8, formazan was recorded using a microplate reader. The percent ratio of the OD value for the dosed cells to that for the undosed cells is calculated and termed as relative cell viability (Figure 2).
24. Lauffenburger DA, Horwitz AF. *Cell.* 1996;84:359.
25. Cells were grown on collagen-1 coated glass cover slips first and then cultured for 16 h in a serum-free medium containing the DMSO solution of compound 7e at 5 μM or a neat DMSO solution in a vehicle control. The cells were then fixed with PFA, permeabilized with Triton X-100 and BSA in PBS. The f-actin in the cells was specifically stained by red Alexa548-phalloidin and nuclei of the cells by blue DAPI, respectively. After the staining, the cells were put under a laser scanning confocal microscope for visualization and the observed images of the cells are shown in Figure 5.